RESEARCH STRATEGY

Background and Significance

***Background**:* The proposed work finds its *scientific premise* *1)* in a rich, century-long literature that characterizes the vibrissotrigeminal system as a model for the study of sensorimotor integration; *2)* in testing an extensive set of recent predictions that have emerged directly from advances in quantifying rodent facial anatomy and whisking behavior; and *3)* in extensive preliminary data demonstrating feasibility of the proposed work.

Over a century of research has established the rodent vibrissal system as one of the premier models for the study of sensorimotor integration, active tactile sensing, and thalamocortical processing[6, 7]. Rats and mice are nocturnal animals with low acuity vision[67-72]. During tactile exploratory behavior, both species often sweep their vibrissae (whiskers) back and forth in a rapid, rhythmic motion called "whisking"[4-7]. As shown in Fig. 1A, about 30 vibrissae are arranged in a regular array (rows and columns) on each side of the face[48, 73]. Vibrissae have no sensors along their length. Instead, the base of each vibrissa is embedded within a densely innervated follicle[74-76], where mechanoreceptors transduce deformations into electrical signals that are sent to the primary sensory neurons of the trigeminal ganglion (Vg)[15, 16, 20, 67, 77-79]. Signals from the Vg then ascend via multiple parallel pathways through the trigeminal brainstem, thalamus, and cortex. In general, the neurons of these pathways are spatially arranged so as to reflect the peripheral facial topography; this arrangement is seen most clearly in somatosensory cortex, where patterns of "barrels" and "septa" distinctly recapitulate the arrangement of whiskers on the face. Our understanding of processing in these neural pathways has increased in concert with our understanding of the peripheral mechanotactile (sensory) signals that drive them[15-17, 20-22, 80-82]. Thus, most generally, the proposed work – which aims to characterize the whisker motor periphery – is premised in a wealth of studies indicating that peripheral morphology and neural processing are closely intertwined. A similar premise underlies studies of the musculature involved in birdsong[83-86].

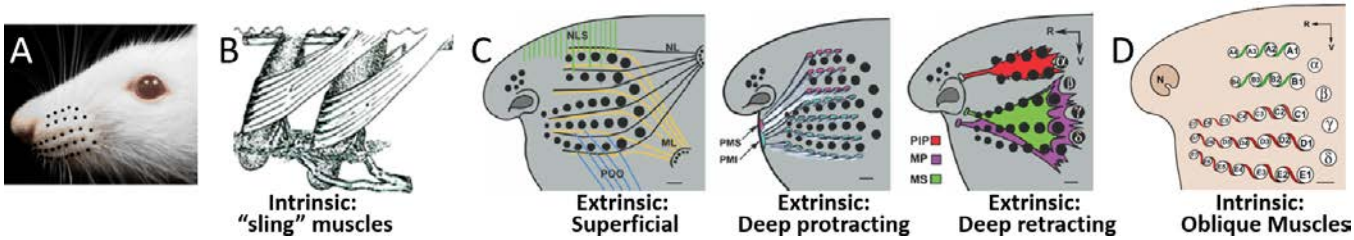

Fig. 1. (A) Vibrissae are regular arranged rows and columns on the rat mystacial pad. **(B)** Intrinsic muscles wrap as "slings" around follicles. From Dorfl, 1982[23] **(C)** Extrinsic muscles are classified as superficial, deep protractors, and deep retractors. Figure adapted from Haidarliu et al, 2010 [25] **(D)** The "oblique intrinsic muscles" are dedicated to generating whisker torsion ("roll"). Adopted from Haidarliu et al., 2017[ref]. Abbreviations and predicted functions are in Table 1.

More specifically, the work is premised on testing a recent set of predictions for the functional roles of different facial muscles. It has been known since 1982[23] that whiskers are actuated by both intrinsic (sling) muscles (Fig. 1B), as well as extrinsic muscles that connect to the skull (Fig. 1C). Recent work has further shown *1)* that each intrinsic "sling" muscle connects two adjacent follicles such that the minimal "unit" of actuation a row-wise pair[61]; *2)* that the extrinsic actuation of vibrissal follicles involves at least ten muscle branches[25, 56, 57, 62, 63]; and *3)* that the oblique muscles (OM) are uniquely dedicated to generating whisker torsion, sometimes also called whisker "roll"[64] (Fig. 1D). *Although the authors of these studies made specific predictions for each muscle's functional role, the predictions were never tested because no 3D model of rodent facial musculature yet exists. The proposed work will directly test these predictions.*

The work is also premised on recent behavioral and neurophysiological results indicating that although whisking is fundamentally a rhythmic behavior, it incorporates a remarkably varied, nuanced movement repertoire. On the one hand, whisking movements are driven by a central pattern generator[24], they have an extraordinarily precise frequency (8 Hz) when averaged over many cycles, and they are often synchronized and symmetric between the two sides of the face[4, 7, 24, 87-90]. Studies that have exploited these spatiotemporal regularities have shed considerable light on vibrissal active touch[1, 4, 89-96]. On the other hand, multiple studies have highlighted the complex biomechanics of whisking and its rich variability during exploratory behavior[26-35]. The dominant rostral-caudal (RC) whisking motion is coupled to changes in dorsoventral (DV) elevation[97] as well as to roll of the whisker about its own axis[98]. Rats can vary whisking amplitude and velocity; whiskers on right and left sides can move asymmetrically and asynchronously[5, 29, 30, 87, 88, 99]; whiskers on a single side of the face have a degree of independence [5, 31-33]; and contact with an object strongly affects subsequent whisking motions[26, 28-30, 99]. This variability in whisking kinematics effectively allows the rat to change the position, shape, and size of the vibrissal

array about its head, and the way that the rat's search space varies across different behavioral conditions is thought to reflect both reflexive components[34, 99] as well as the process of directed attention[30]. Whisking provides a unique window into how neural control can modulate or override centrally-patterned movement and is an ideal behavior to "close the loop" between sensory and motor structures. The proposed work is premised in identifying which components of whisking are biomechanically constrained, which are driven by the CPG or reflexes, and which are under more voluntary neural control.

Significance: Completion of the work will have significant impacts within the field of vibrissal research, and more generally on our understanding of the neuromechanical basis for sensorimotor control. ***1)*** Identifying the degree to which different features of whisking are biomechanically fixed, versus which are neurally controlled, will directly constrain how the nervous system achieves descending control of whisking motions. This knowledge is important for all researchers working on vibrissal-related motor structures, including regions of motor thalamus and cortex; motor regions of the brainstem; superior colliculus; crus I, crus II, and crus IX of the cerebellum and the deep cerebellar nuclei to which they project; striatum and basal ganglia. All of these structures send significant motor outputs to the whiskers, yet we have not yet even identified the mechanical function of their ultimate peripheral targets. The proposed work will aid investigation of these structures. ***2)*** The proposed work will quantify the patterns of muscle activation that underlie changes in whisking parameters. These results will in turn inform researchers how rodents might change whisking motions to optimize the acquisition of particular types of sensory information for a given behavioral task. This knowledge is important both for researchers working on vibrissal-related sensory regions, including barrel cortex, as well as for researchers who study reward circuitry and the energy-information tradeoff. ***3)*** Developing mechanical models has already had a demonstrated, significant impact on the field of vibrissal sensory research. Starting in 2006, the first models of sensory (tactile) vibrissal mechanics[37, 38] gradually led the field to begin to quantify vibrissal sensory signals in terms of mechanical variables[8, 15-17, 20]. The proposed work now takes a similar approach in performing mechanical modeling of the muscles involved in whisking. We anticipate these models will have a similarly significant effect on the field. ***4)*** From the clinical side, the transition between varieties of rhythmic and non-rhythmic movement has important implications for the coordination of sniffing, breathing, olfaction, chewing, swallowing, and suckling. The proposed work could shed light on the neuromechanical basis for some pediatric and geriatric dysphagias.

Innovation**:** The work has several innovative aspects: ***1)*** The work develops the first-ever 3D models of the facial musculature that controls vibrissal motion. ***2)*** The field of vibrissal research is largely (though not entirely) focused on the tactile signals acquired by the whiskers. The proposed work is innovative in focusing on the direct mechanism of actuation by which these tactile signals are acquired, that is, in constructing muscle models for a "sensory" behavior. ***3)*** The proposed work is innovative in establishing the vibrissal system as one of the few models (perhaps the only mammalian model) for which we can simultaneously quantify both the sensory input (tactile signals at the base of each whisker) and the patterns of motor actuation that directly drive the acquisition of those sensory signals. ***4)*** We think it natural that the study of human sensorimotor performance benefits from systems such as OpenSim[100], software specifically designed to model human musculoskeletal biomechanics. OpenSim has successfully allowed researchers to study the mechanisms that underlie human movement disorders, and to evaluate the parameters that maximize motor performance. Yet we have no such software available for rodents – the most common animal model used in all of biomedical research. The proposed work is innovative in asking "why not?" and then working to develop such software. ***5)*** The work employs a novel combination of four technical approaches for anatomical quantification of the follicles and musculature.

Preliminary data and toolsets: Preliminary data will be described in more detail within each aim. Because my laboratory has worked for the past decade to develop mechanical models of vibrissotactile sensing, we have developed several unique toolsets that we can exploit for the present work. All tools are publicly available.

Toolset 1) We have developed accurate models of the 3D morphology of rat and mouse vibrissal arrays. In 2011 we published our first model of the 3D morphology of the rat vibrissal array[48], using data taken with a laser scanner (Fig 2, left). Last year we improved the model using data obtained with a Microscribe™, a commercial 3D tactile profilometer[45]. Microscribe data offer the same or better resolution than those from the laser scanner, but are easier to analyze because no point-cloud segregation is required[45]. Aim 1 therefore uses the Microscribe for "ground truth" measurements for vibrissal and mystacial pad geometry to compare with MRI and Micro-CT data. Models for both rat and mouse[47] are shown in Fig. 2. The models provide equations

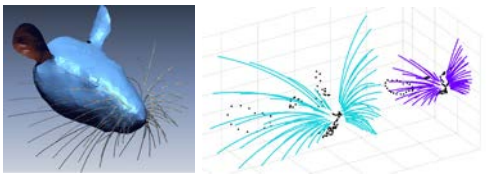

Fig.2. 3D morphology of vibrissal array of a rat using a laser scanner (left) and the Microscribe (right) for rat and mouse. The models provide equations that describe the location of each point on each whisker relative to facial and skull landmarks.

that describe the location of every point on every vibrissa relative to facial and skull landmarks, and have already enabled multiple studies that quantify rat exploratory behavior[51-53, 101-104].

Toolset 2) We have characterized the detailed geometry, mechanics, and material properties of individual rat whiskers in unprecedented detail. We recently finished a meta-analysis of the geometry of 519 rat whiskers from seven different laboratories, quantifying diameter, taper, arc length, and medulla geometry[46]. We then used these measurements to quantify the whisker's center of mass, mass moment of inertia, radius of gyration, and deflection under gravity[49]. We will use these geometric and mechanical results in simulations of the mechanosensory signals associated with vibrissotactile exploratory behavior in Aim 3.

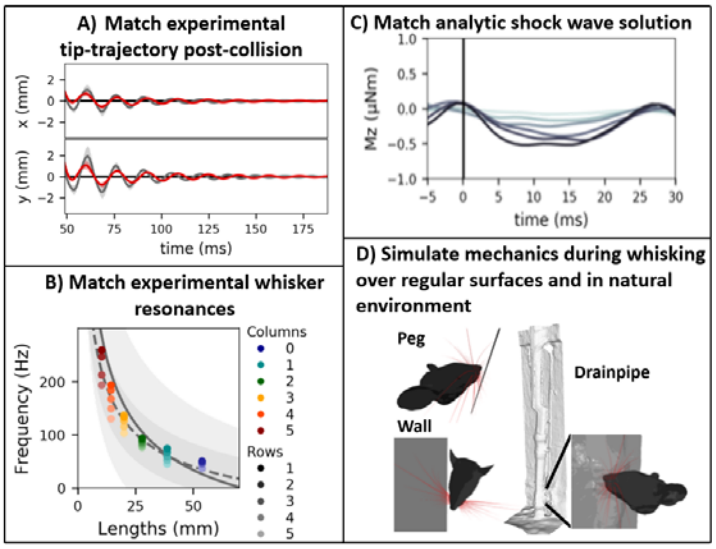

Fig. 3. *Bullet* model of vibrissal mechanics validated against experimental data. **(A)** Post-collision tip trajectory matches between model (red) and experiment (black) **(B)** Simulated whisker resonances match experiment. **(C)** Model matches analytic solutions for a shock wave. **(D)** We can simulate array dynamics during whisking against geometric objects and in natural environment (e.g., a drainpipe).

Toolset 3) We have published models for vibrissal mechanics in multiple simulation environments, including MATLAB™, Open Dynamics Engine (ODE), TREP, and Bullet [15, 43, 52-55, 104, 105]. Our 3D quasistatic model, which can predict all six components of force and moment at the whisker base as the whisker bends against an object, is well-validated and has been used in multiple publications[15, 52, 53, 104, 105]. We have also published a model of whisker dynamics based on a variational integrator approach[43] and used it to show that when an animal whisks against an object the mechanical signals depend critically on the animals' active control over vibrissal deceleration and bending. These results will be important in Aim 3A, when we examine the reflex responses responsible for fast whisker retraction. Most recently, we published a *Bullet*-based model of the complete vibrissal array[54, 55] and, as seen in Fig. 3., have now validated its mechanics against multiple sets of experimental data, including non-contact whisking, whisker resonance, and collisions, as well as the analytic solution for shock wave propagation. In Aim 3, we will combine the muscle model with this model of vibrissal dynamics, thus closing the loop between actuation and sensing.

Toolset 4) We have 3D tracking algorithms. We have several published studies that demonstrate 3D tracking of individual vibrissae during active exploration[52, 105]. In addition, we can now reconstruct 3D head and whisker trajectories of both rats and mice exploring a volume of space using high speed multi-camera videography and DeepLabCut[3] (Fig. 4). The information from many cameras is merged to form a 3D model of the head and whisker kinematics in every frame. We can thus track head and whisker trajectories in unsupervised fashion and dissect the behavior of rodents performing a variety of tasks.

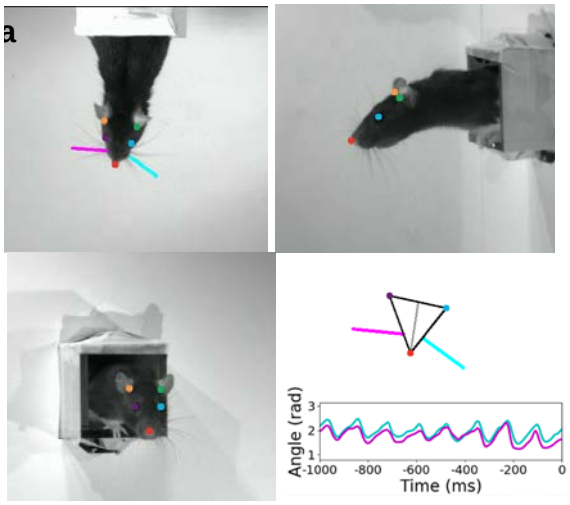

Fig. 4. Unsupervised markerless tracking of head kinematics and whisking motions in 3D. An example 3D pose is shown for a rat with three cameras capturing the head orientation at the same instant in time. Superimposed on the images are automatically detected facial features (nose, eyes and base of ears), shown in different matching colored circles. Whisker arrays mid-positions are also superimposed on panel a and shown as colored lines. Reconstructed head pose and whiskers are plotted in the last panel, along with the whisker angles over the previous 1 second.

Approach

All studies are performed in full accordance with guidelines for protections for animals and approved in advance by the Institutional Animal Care and Use Committee (IACUC) of Northwestern University. We are fully committed to sharing models and experimental data (see *Resource Sharing Plan*). To ensure the broad utility of our mechanical models throughout the field of vibrissal research, the work of Aim 1 and Aim 2 will use both rats and mice. Mice are commonly used in head-fixed behavioral tasks and allow use of a powerful genetic toolset, but many researchers use rats because they are larger and easier to train in complex behavioral tasks. As will be described for

each aim, our experimental and modeling approaches ensure *scientific rigor* through use of appropriate statistical analyses and use of multiple validation methods. *Sex as a biological variable* (SABV) is addressed by using equal numbers of male and female animals in all experiments.

Fig. 5. provides an overview of the proposed work. Quantifying follicle and mystacial pad anatomy (Aim 1) will proceed in parallel with construction of the initial muscle model (Aim 2A); anatomical features will be incorporated into the model as they are revealed. The muscle model will be tuned and tested experimentally against specific functional predictions for muscle function (Aims 2B and 2C), and ultimately used with our established models of vibrissal sensory mechanics[15, 43, 52-55, 104, 105] to explore hypotheses for closed-loop sensorimotor control (Aim 3).

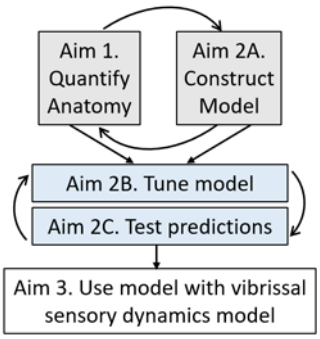

Fig. 5. The proposed work contains two pairs of Aims (1 & 2) that iterate between model and experiment, culminating in closed-loop sensorimotor simulations (Aim 3)

Aim 1: Quantify key elements of the 3D anatomy of the mystacial pad musculature and follicles. Previous studies have provided excellent descriptions and schematics of muscle anatomy[25, 56-66], but we lack critical quantitative data needed to construct a 3D muscle model. We will use a novel combination of tactile profilometry, histology, MRI, and micro-CT to *meet the need* for accurate anatomical models.

Overview of Aim 1: Adult (>3 mo.) rats and mice will be used in these experiments, with equal numbers of males and females of both species. We exploit tradeoffs in four complementary technical approaches to quantify the 3D shape, position and orientation of the follicles and the intrinsic (sling) muscles, as well as the 3D geometry of the extrinsic muscles and their attachment points on the skull. MRI and CT-scan data will be obtained at Northwestern's Center for Advanced Molecular Imaging (CAMI):

- *3D tactile-profilometry with Microscribe™:* Tactile profilometry in the anesthetized animal ensures that tissue does not distort, however, these measurements are limited to the outside of the animal. We can directly measure 3D facial landmarks, whisker orientations and basepoints, but follicle orientations must be inferred from the angles of emergence of the whiskers.
- *Histology:* The histological approach allows us to precisely quantify 3D follicle and intrinsic (sling) muscle geometry, however, the fixative process can cause distortion and shrinking. We can correct for this distortion by measuring sarcomere length, by scaling the basepoints of the follicles to align with the basepoints measured with the Microscribe, and by aligning muscle geometry with MRI.
- *MRI:* These experiments will be performed in the anesthetized animal, and our preliminary data (Fig. 6) already demonstrate the feasibility of extracting the 3-D geometry of intrinsic muscles. The resolution of MRI is lower than that of micro-CT, but it provides accurate geometry of the anesthetized animal against which the higher resolution data (from micro-CT or histology) can be registered.
- *Micro-CT:* The *in-vivo* micro-CT system at CAMI will permit scans with a spatial resolution of ~50 µm.

Importantly, we can use all these techniques in the same individual animals. An experiment will begin with tactile profilometry and/or MRI and *in vivo* CT scans of the anesthetized animal, followed by histology. Images from all four techniques can be registered with Amira software. Cross-validating alignment across these multiple methods helps ensure *scientific rigor* for Aim 1.

Aim 1A. Quantify 3D follicle geometry across the mystacial pad with histology and tactile profilometry. Fig. 6 shows preliminary data illustrating the procedure. Mystacial pads will be cryoprotected, flash-frozen, sliced (20 or 40 µm), and slide mounted (Fig. 6A). Phosphotungstic acid haema-toxilin (PTAH) will stain muscles and

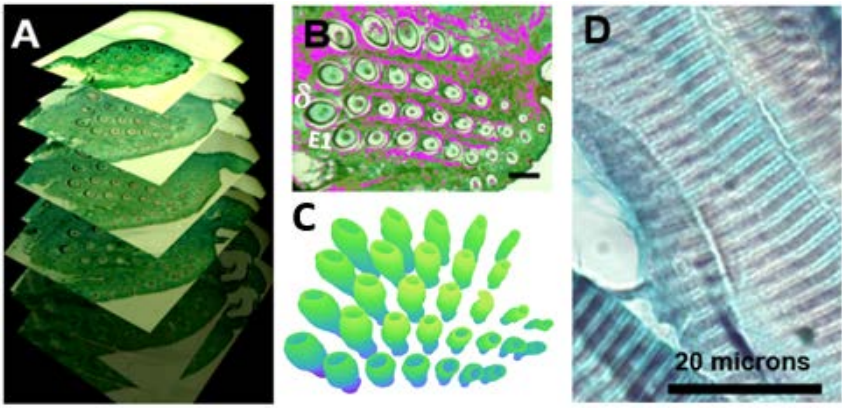

Fig. 6. Follicle and muscle anatomy (A) Aligned stack of tissue sections. **(B)** A section of a whisker pad with FG-stained collagen (green) and PTAH-stained muscles (pink). The A-row is missing in this slice. The δ and E1 whiskers are indicated for reference. **(C)** Elliptical outlines of each follicle in each slice are stacked to reconstruct 3D follicle geometry. **(D)** Intrinsic muscle fiber tissue stained with PTAH, showing striations.

fast green (FG) will stain collagen (Fig. 6B). Sections will be photographed at 8x magnification to create an aligned "z-stack." The outline of each follicle will be traced in each tissue section and fit with an ellipse in MATLAB. When stacked, these elliptical outlines form a full 3D representation of each follicle and its orientation within the pad (Fig. 6C). We will quantify the long and short axes of each follicle, the angles of each follicle relative to each other and to the skin, and the diameter as a function of position along the length of the follicle.

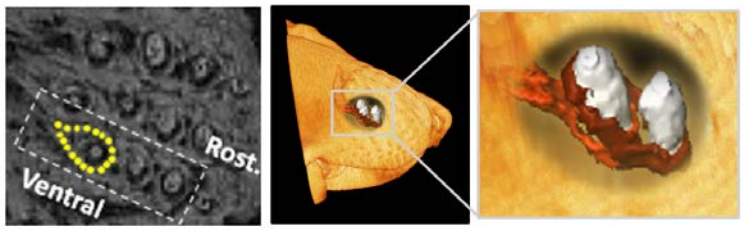

Fig. 7. Left: A slice from an MRI in the euthanized animal obtained with a fast T1-weighted protocol. Image quality will improve in the anesthetized animal and with use of T2-weighted, turbo spin echo, but even this sub-optimal image permitted reconstruction of two follicles and sling muscles (Right).

Two controls will help exclude artifact due to mechanical deformation in the tissue preparation process. First, as shown in Fig. 6D, PTAH stains muscle striations, so we can measure the average sarcomere length of the intrinsic muscles at different positions in the mystacial pad. Given that most intrinsic fibers are all of the same type (2b)[106], the average sarcomere length should be the same across the whole pad if minimal deformation is present (*i.e.,* if relative follicle orientations are accurate). Second, prior to perfusion, follicle spacing at the skin surface and the curvature of the mystacial pad will be quantified using the Microscribe 3D tactile profilometer (see Fig. 2). We will scale the histological tissue to these measurements.

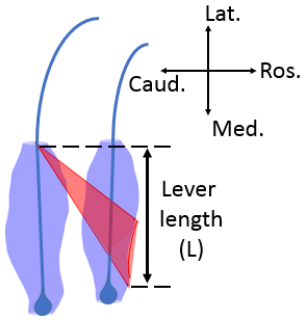

Fig. 8. The lever length (L) of a sling muscle can be determined by finding its medial and lateral extent in histology sections, and through MRI.

Aim 1B. Quantify intrinsic muscle geometry and force generation from MRI, micro-CT and histology. We will obtain an initial estimate of 3D intrinsic muscle geometry by performing MRI experiments at CAMI. MRI has relatively low spatial resolution (~100 μm) but can be performed in the anesthetized animal, eliminating the global fixation distortions associated with histology. Histological data are higher resolution, and can be aligned with the non-distorted MRI data to improve estimates. In preliminary work we have obtained an MRI slice through the follicle pad of a euthanized rat taken with a fast T1-weighted protocol (Fig. 7, left). In this particular slice, intrinsic muscles are clearly seen around three ventral follicles in the E-row, while more dorsal intrinsic muscles are out of the plane. Contrast will improve in the anesthetized animal and with use of a T2-weighted, turbo spin echo image. Nevertheless, even in this non-optimized image it is clear that the whisker follicles and intrinsic muscles wraps are easily seen and the follicle apex and base can be traced. The right panels of Fig. 7 show reconstruction and surface rendering of two follicles and sling muscles using Amira software (FEI, Burlington, MA).

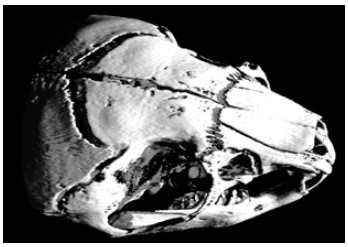

Fig 9. (A) 3D Lab micro-CT rendering of a juvenile murine skull. Data obtained at station 2-BM, Argonne, by Drs. SR Stock and CP Richter, used with permission.

Following the MRI experiment, we will perform *in vivo* micro-CT to obtain an estimate of 3D skull geometry, followed by histology to obtain high resolution geometry of the muscles. All results will be carefully compared with those of Kim et al., who have performed a similar analysis for a single row of vibrissae [59, 60]. Examination of sequential histological sections will determine lever length L, identified in Fig. 8. After registering the data between the three techniques, an estimate of muscle force will be obtained using the muscle cross sectional area and fiber length. Optimal sarcomere length is known from the literature (2.4 - 2.64 μm)[107]. These parameters are sufficient to estimate muscle force[108], which will be use in the model of Aim 2.

Aim 1C. Quantify the 3D geometry of the skull and extrinsic muscles from micro-CT, and extensive descriptions from the literature. We will quantify the 3D geometry of multiple adult rat skulls using micro-CT, which will also identify the attachment points of the extrinsic muscles (Fig. 9). We can then fit the shape of the mystacial pad as determined from MRI and the Microscribe curvature measurements from Aim 1A. We have not yet tested the micro-CT facilities available at CAMI; the Fig. 9 preliminary micro-CT data are from our work with Argonne National Laboratories. We plan to use the CT facilities at CAMI because they are closer to our laboratory, and because we anticipate the resolution will be adequate. However, if we need higher resolution, we will return to our work at Argonne (see "alternatives"). We will combine the quantified attachment points from the micro-CT with the detailed descriptions and illustrations of attachment points for all extrinsic muscles available in the literature [25, 56, 57, 61, 109], and Microscribe profilometry to develop and tune the model in Aim 2.

Aim 1: Predicted outcomes, potential challenges, and alternatives. Combining the four technical approaches gives us confidence that at the end of Aim 1 we will have obtained high quality reconstructions of the 3D anatomy of the mystacial pad musculature and follicles. We anticipate that we will obtain sufficient resolution for the intrinsic muscles by combining histology and MRI, and sufficient resolution for the extrinsic muscles and their attachment points by registering MRI with micro-CT, guided by detailed descriptions from the literature[25, 56, 57, 61, 109]. We also anticipate that CAMI facilities will provide adequate resolution for the CT-scans, however, if higher resolution is required, we will take advantage of the PI's previous work with researchers at Argonne National Laboratories and Northwestern's close relationship with this facility[110] to obtain higher resolution CT-scans (~1 - 10 microns). The image shown in Fig. 9 was in fact taken using the 2-BM beamline at Argonne. This technique will allow us to obtain 3D geometry of the skull and entheses and then register the high resolution images with lower ones.

To further ensure the ***scientific rigor*** of Aim 1 we determined the number of animals required using power analyses for regression models. This statistical approach is appropriate because the proposed research involves descriptive modeling rather than experimental manipulation and hypothesis testing. Power analyses were conducted using the statistical computing software Gpower[111] assuming an alpha of 0.05 and a beta of at least 0.8. We tested a range of effect sizes (Cohen's F) calculated from the model R^2 from published measurements of rat and mouse whisker morphology[45, 47] and from preliminary data on rat whisker follicle morphology (Fig 5). The lowest R^2 found was for resting whisker orientation and was 0.34 for mice and 0.42 for rats. However, these R^2 values were by far the lowest, and if they are excluded as outliers, the next lowest R^2 value found is 0.55. Using this more probable value, and estimating that confounding variables such as sex contribute to ~50% of the variance, the predicted sample size is ~15 (7-8 males and 7-8 females) for each species. The highest R^2 found was 0.95, yielding a predicted sample size of 8 (4 males and 4 females), providing a lower bound on the number of animals needed. We therefore propose to use 15 rats and 15 mice, but may reduce this number if preliminary models show a large effect size.

Aim 2: Construct a 3D model of the mystacial pad musculature and follicles to simulate motion of the vibrissal array. We do not aim for an exact model, but rather one that can tell us about relative functional relationships between muscles. The model will be closely based on papers by Haidarliu et al.,[25, 56, 57, 63, 64] and gradually incorporate the new anatomy of Aim 1. We will use high-speed 3D kinematic analysis to constrain the model and ***test eleven specific predictions of previous studies.***

Overview of Aim 2: Haidarliu et al., 2011[57] and 2017[64] performed detailed microanatomy of the rat mystacial pad, identified eleven muscles involved in vibrissal motion, and made predictions for each muscle's functional role. The authors summarized their findings in a schematic, but the *model itself was never created, and the predictions were never tested.* An annotated version of the Haidarliu schematic is shown in Fig. 10, and the muscles listed in Table 1[25].

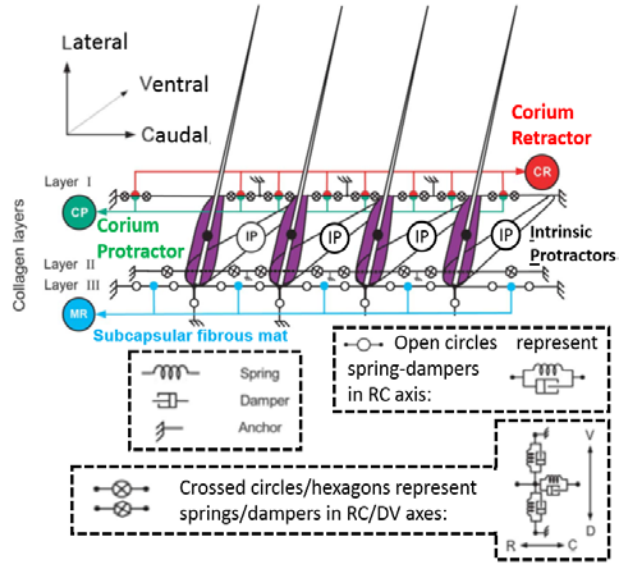

Muscle	Expected effect
Nasolabialis	Pull the corium of the mystacial pad dorsocaudal. Vibrissa retraction
Maxillolabialis	Pull the corium of the mystacial pad ventrocaudal. Vibrissa retraction
Nasolabialis superficialis	Pull the corium dorsally. Elevate vibrissal rows A and B.
Buccinatorius Pars orbicularis oris	Pull maxillary subdivision of the mystacial pad downward. Ventrocaudal deflection of vibrissal rows C–E.
Nasolabialis profundus (NP) Pars media superior	Rostral pull of corium of the nasal subdivision of the mystacial pad. Protraction and convergence of vibrissal rows A and B.
(NP) Pars media inferior	Rostral pull of corium of the maxillary subdivision of mystacial pad. Protraction and convergence of vibrissal rows C – E.
(NP) Pars interna profunda	Rostral pull of the plate. Retraction of vibrissal rows A and B
(NP) Pars maxillaris superficialis	Pull the plate rostral. Retraction of vibrissal rows C–E.
(NP) Pars maxillaris profunda	Pull the plate rostral. Retraction of vibrissal rows C–E.
Intrinsic muscles	Rostral [caudal] pull on distal [proximal] ends of follicles and corium Follicle rotation about DV axis, whisker protraction.
(OM) Intrinsic oblique muscles	Torsional motion of the whiskers.

Table 1. Eleven functional predictions for model. From Haidarliu, 2010 and 2017 [64]. Abbreviations: NP: nasolabialis profundus. RC: rostro-caudal. DV: dorso-ventral.

Fig. 10. Annotated schematic from Haidarliu et al., 2011.[57] The model has attachment points in three layers. The oblique muscles (OM) that generate torsion are not shown.

Choice of modeling software: The internet is replete with heated debates over which physics engine is "best." The answer is that "best" depends on the particular modeling questions being asked, and on the desired features for the model. For work as complex as that described here, we fully anticipate using multiple software packages for model validation, prior to testing against experiments. Our laboratory has extensive dynamic modeling experience, having published models using *MATLAB™, Open Dynamics Engine (ODE), TREP, and Bullet*; we also have some experience with *OpenSim*. The final model of the rat facial musculature will be developed in Bullet[112], which offers several advantages: *1)* models with complex, arbitrary geometry can be rapidly constructed; *2)* simulations are fast; *3)* simulations will interface seamlessly with our existing, experimentally-validated Bullet model of 3D whisker dynamics (Fig. 3). The main disadvantage of Bullet is that its underlying equations do not fully guarantee dynamically-accurate results under all conditions. Therefore, each step of the proposed work takes pains to ensure dynamic accuracy of the simulations. To do this, key components of the models will be tested against TREP, and against OpenSim[100]. Notably, this type of modeling approach has worked well for our models of vibrissal sensory dynamics (Fig. 3)[43, 54, 55]. TREP offers a validated variational integrator approach[113-117] [43] that fundamentally guarantees conservation of energy and momentum, but collision detection is challenging and the runtime is relatively slow: TREP is extremely accurate at the expense of simulation flexibility. OpenSim offers exceptional tools for simulating musculoskeletal biomechanics and is generally thought to be dynamically accurate, but it is focused entirely on human biomechanics and its complexity will be "overkill." Validation of the facial musculature model across multiple physics engines (Aim 2A), coupled with the integration of experimental data (Aim 2B) and testing against experimentally-measured kinematics (Aim 2C) ensures the *scientific rigor* of the work proposed in Aim 2.

Aim 2A. Develop a model of facial musculature that incorporates 3D follicle and muscle geometry. We will use the anatomy of Aim 1 to incorporate follicle lengths, diameters, and spacings, as well as curvature of the mystacial pad and 3D muscle geometry. The model will include all three collagen layers from Haidarliu et al., 2011[57] and will permit rostral-caudal (RC), dorsoventral (DV), and mediolateral (ML) movement. Implementing these layers in Bullet is not a challenge – instead, the critical feasibility demonstration is that the *most accurate* dynamic model has the capacity to converge to a physically reasonable solution. In preliminary work, we therefore implemented the 2D Hill et al. 2008 muscle model[58] within the TREP dynamic simulation environment. The model is shown in Fig. 11. When both models are tested with identical muscle inputs (Fig. 11B) the angles match to within 0.014 degrees for all follicles, and the x-position of the center of masses match to 5×10^{-4} mm. These tiny disagreements occur primarily because the models use different differential equation solvers.

Aim 2.A.1. Incorporate correct inter-follicle spacing and follicle length. As noted in Background and schematized in in Fig. 8, previous studies have demonstrated that intrinsic muscles within rows connect two adjacent follicles such that the minimal actuation "unit" is a row-wise pair [61]. The muscle stretches from the apex of the caudal follicle, to loop around the rostral follicle just above its base. The lower border of this muscle loop defines a "lever" (the lever length, L), by which that muscle moves the associated whisker. The lever length is not exactly the same as the follicle length, because the very basal portion of the follicle (important for whisker growth) is below the attachment point of the muscle (see Figs. 1B and 8) This geometry has important consequences for whisker movement, as schematized in Fig. 12. Trigonometric analysis shows that the ratio of the separation between the follicles (S) and the lever length L will have a dramatic influence on the motion of the whiskers. Any non-constant S/L ratio will cause the whiskers to move through larger angles from caudal to rostral. Importantly, this differential movement is not always observed during natural behavior[26, 27], suggesting a high degree of volitional control over the spread of the whiskers.

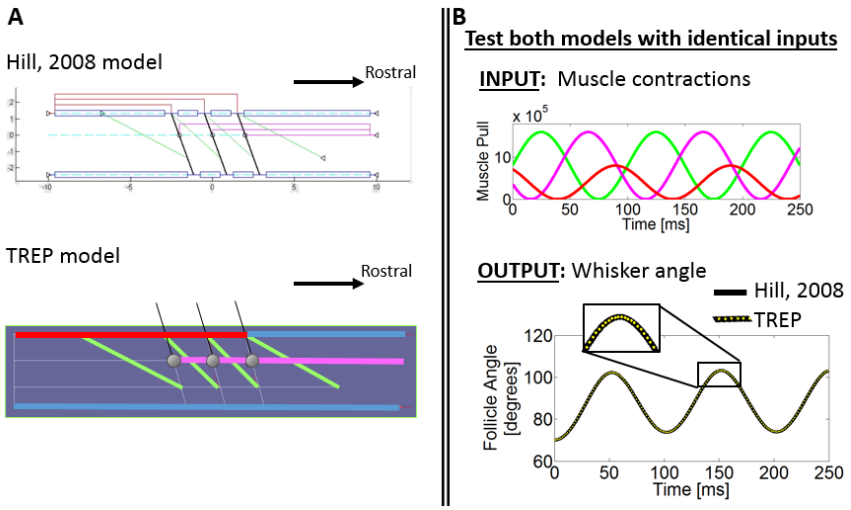

Fig. 11. (A) Hill et al. 2008 model (upper schematic) is implemented within TREP (lower schematic) **(B).** When both models are provided with the same muscle inputs (upper), the outputs match to within precision of the differential equation solver. Muscle contractions have been normalized according to muscle length, following the procedure of Hill et al., 2008.

Aim 2.A.2. Incorporate correct follicle orientation and mystacial pad curvature. The curvature of the skin surface can be obtained by fitting a

surface to the most lateral surfaces of the follicles. The mystacial pad curvature can also be confirmed with the Microscribe in anesthetized rats to eliminate distortion due to fixation.

Aim 2.A.3. Incorporate intrinsic and extrinsic muscles. The geometry of both sets of intrinsic muscles ("sling" and oblique), and the locations at which they pull the follicle, will have been determined in Aim 1. To incorporate the effects of the "sling" muscles, the whisker's roll about its axis will be modeled as two coupled spring-damper muscles, acting on dorsal and ventral follicle surfaces. The oblique muscles will be modeled as single spring-dampers that pull dorsocaudally for rows A and B and ventrocaudally for rows C- E (see Fig. 1). Contraction of the these muscles will be differentially varied to match experimentally magnitudes of roll[98] in Aim 2B. To incorporate the effects of the extrinsic muscles with multiple attachment points will require careful analysis of "lines of action" (the geometry through which the forces act) using the micro-CT data. At each inflection point we will identify the location and direction(s) of force, allowing extrinsic muscles to pull in parallel, on multiple follicles simultaneously.

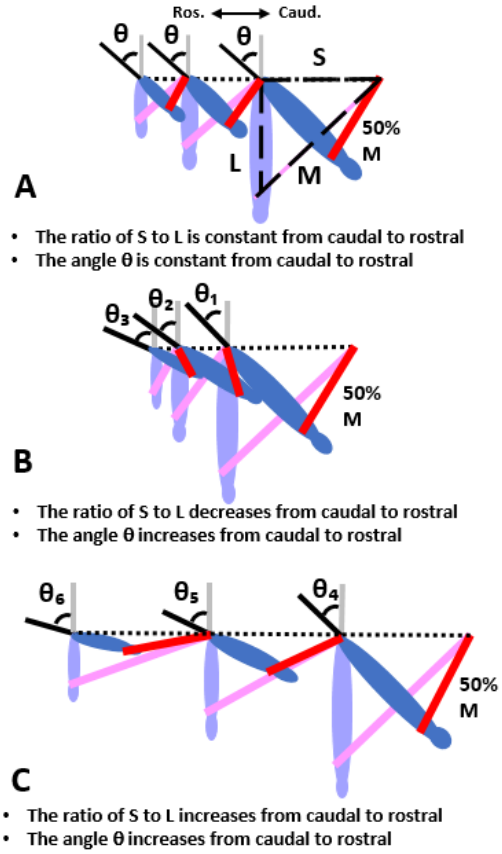

Fig. 12. Any non-constant S/L ratio will cause the whiskers to move through larger angles from caudal to rostral

Aim 2A: Expected outcomes, potential challenges, and alternatives: By the end of Aim 2A we will have established a 3D model of mystacial pad musculature that incorporates all known features of the anatomy from the literature and Aim 1. Movement in the primary direction of whisking motion (rostral-caudal, RC) will be driven by both intrinsic and extrinsic muscles. Elevation movements in the dorsal-ventral (DV) direction will be almost exclusively driven by extrinsic muscles, however, intrinsic muscles could have a small influence if their 3D orientation is found to be tipped in the DV direction. In contrast, roll about the whisker's own axis will be driven exclusively by the two sets of intrinsic muscles, as there is no evident biomechanical means for the extrinsic muscles to contribute. Finally, movement in the medio-lateral (ML) direction, perpendicular to the animal's cheek, will result from intrinsic muscles and the stiffness of the layers in RC and DV directions. Because each of these 3D movements is driven by differential combinations of extrinsic muscles, we can use kinematic analysis to constrain and tune the model, as described next in Aim 2B. The primary challenge for Aim 2A lies in ensuring that our simulations are dynamically accurate while also computationally tractable. This challenge will be addressed by cross-validating Bullet simulations with results from multiple physics engines, as described in "choice of software." As shown in Fig. 3, this approach has worked well for our model of vibrissal dynamics[55].

Aim 2B. Use high-speed 3D kinematic analysis and EMG recordings to constrain the model. Kinematic analysis alone cannot uniquely determine muscle forces, but it can constrain relative forces exerted by muscles with different lines of action. The combination of kinematic analysis, EMGs, and lesion experiments can be enough to determine relative muscle contributions to specific motor patterns[113].

Aim 1 quantified anatomy for both rats and mice, and Aim 2A developed a model for both rats and mice. However, Aims 2B and 2C will be performed for the rat only because rats are larger and easier to observe and train. Equal numbers of adult male and female rats will be used. The final model of Aim 2 will then be scaled down and adjusted for the mouse to incorporate any differences in anatomy revealed by Aim 1. Select experiments might be performed on the mouse on an as-need basis. Although the novelty of the work makes it challenging to predict exactly how many animals will be required, our laboratory's previous behavioral studies have all used between 3 – 8 animals [34, 35, 51, 102, 118]. We anticipate similar numbers for each of the four muscle groups described in Aim 2.B.3 below for a total of 12 – 32 animals over the 5-year period.

Aim 2.B.1. Perform experiments to obtain kinematic and EMG data. Tools already established in our lab (Fig. 4) allow us to merge views from three video cameras to quantify 3D kinematics in freely whisking rats and mice. We will quantify *1)* row-wise (or column-wise) kinematics by completely trimming all whiskers except in one row (or column) and *2)* elastic deformation of the mystacial pad, by tracking relative 3D basepoint positions. Simultaneous EMG recordings will also help place constraints on the model, as shown in Fig. 13. This figure depicts summed, normalized[58] EMG signals from an extrinsic muscle (most likely *NP Pars maxillaris profunda*)

synchronized with mystacial pad movement and the whisking cycle. All EMG locations will be verified by passing current through the EMG wires to stimulate the muscles and confirm recording sites[58]. We will record from both extrinsic and intrinsic muscles, using procedures described in Hill et al., 2008[58].

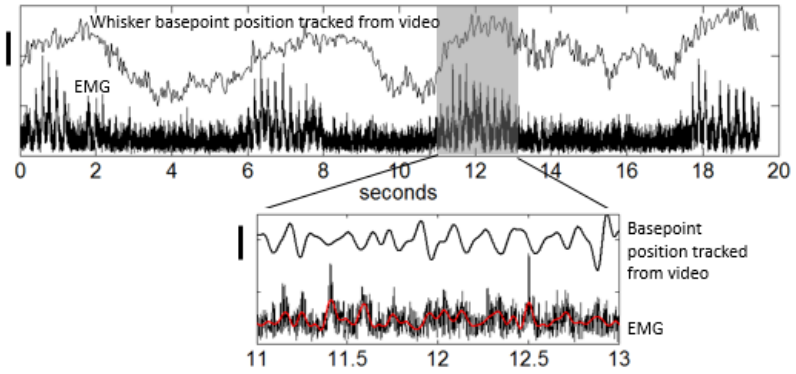

Fig. 13. ~20 seconds of ∇EMG signals from a whisking rat, with EMG electrode most likely in *NP Pars maxillaris profunda* (see Table 1). Top trace represents tracked basepoint of the D1 whisker. Scale bar ~500 μm. Lower trace represents the normalized ∇EMG signal filtered at 300 Hz. (units arbitrary, following conventions of Hill et al., 2008). Low frequency component of the EMG follows low frequency motion of mystacial pad. **Expanded plot** shows that the higher frequency component of the EMG follows ~8 Hz whisking motion. Top trace again represents motion of the D1 basepoint; scale bar ~200 μm. Lower trace is the ∇EMG signal. **Note:** the behavioral traces in both subplots represent vibrissal basepoints, not whisker angles. The whisker angle would have larger amplitude near 8 Hz. This figure demonstrates we can monitor basepoint movements, a even more challenging problem than monitoring whisker angles.

Aim 2.B.2. Model the kinematic and EMG data. Our approach to modeling the vibrissal array is based on the insights that *1)* the mystacial pad is fundamentally constrained to the shape of the rat's face, and *2)* conformational changes of the mystacial pad do not induce large changes in the dynamics. The relative dynamic invariance of the rat vibrissal array is what makes our modeling approach fundamentally tractable. Modeling muscle dynamics involves two closely-related challenges. The first challenge is to determine the magnitude and direction of the effect that each muscle has on each individual vibrissa. This is a difficult problem because there are many muscles but only three resultant forces and three resultant torques at the base of the vibrissa. An initial analysis of kinematic data can constrain the sum of forces acting on the whisker, while taking into account the geometry through which forces act on vibrissa. Next, as indicated by the "expected actions" of each listed in Table 1, we note that each muscle is likely to have *one or more components of force that act independently of the other muscles.* This independence then permits pseudo-inverse techniques to be used to provide least-squares estimates of the individual muscle formulas[119-121]. Importantly, even without EMG recordings, one can approximate the relative contributions from each muscle by using relative force generation capacity (Aim 1), and assuming that the muscles will be used optimally during motion. The key is that one can reconstruct estimates of individual muscle activity directly from kinematic data so long as the kinematics can be related to the **net** force and moment vector (all six components) at the base, and as long as the muscles exert at least some non-independent forces on the follicles. The second challenge, to be addressed iteratively with the first, is to determine the density, elasticity (spring constant), and damping associated with each muscle and mystacial pad tissue. Several previous studies have provided reasonable estimates for skin and muscle elasticity and damping; these values are consistent with estimates from human skin, which is well-studied by the cosmetics industry. These numbers will allow us to bootstrap simulations into a physiological-plausible range.

Aim 2.B.3. Integrate experimental data into the model and tune the model. We will use the following four measurements to constrain functional activation of muscles in the model:

- *Relative magnitudes of elevation and roll constrain relative activation of extrinsic and intrinsic muscles:* Movement in the DV plane is driven almost entirely by extrinsic muscles, while roll of the whisker about its own axis is driven by intrinsic muscles. We will therefore match elevation with extrinsic activity alone, match vibrissal roll with intrinsic activity alone, and then differentially vary the relative magnitudes to generate observed trajectories[98].
- *Relative magnitudes of translation and rotation constrain relative extrinsic/intrinsic activation:* Basepoint translation is driven almost entirely by extrinsic muscles, while rotations are generated primarily by intrinsics. We will match translation using extrinsic contractions alone, and then differentially vary relative intrinsic-extrinsic magnitudes to match both translation and rotation kinematics[25].
- *Deformations of the mystacial pad constrain extrinsic contractions:* Relative motion of the basepoints in 3D and the whole pad's position and angles relative to the RC/DV axes provide constraints on relative contractions of extrinsic muscles.
- *Phase lead of the rostral compared to caudal vibrissae*: A rostral vibrissa phase lead is seen in many behaviors[122], suggesting a biomechanical constraint on the contraction of intrinsic muscles within a row.

Aim 2B: Expected outcomes, potential challenges, and alternatives: Aim 2B merges experimental data into the model to specify the relative muscle contributions to specific motor patterns – in other words, Aim 2B "tunes" the model using experimental data. Importantly, however, the model could theoretically be tuned in very non-realistic ways. We reiterate (see overview, Fig. 5) that Aim 2B will progress iteratively with Aim 2C, which performs experiments to test the function of each muscle for any given tuning suggested by Aim 2B. To ensure tractability, we will not attempt to tune and test all muscles simultaneously, but rather split the problem into the muscle groups indicated by the kinematic relationships identified in Aim 2.B.3. Group will be combined to form the full model. In general, all of these experimental and modeling approaches are established in our laboratory, however, one challenge is that the roll of the whisker about its own axis is often difficult to measure. We have successfully measured 3D roll in published work[53], and we can also take two cross-validating approaches to this challenging problem. First, we can leave enough of the whisker length to quantify roll based on apparent changes in intrinsic curvature between the cameras. Second, the whiskers can be trimmed, their insertion into the follicle exposed with depilatory cream, and three points along their length marked with reflective dye[98].

Aim 2C. Test the eleven predictions of Table 1. Aim 2B will have already integrated experimental data into the model in order to arrive at a set of plausible tunings for each muscle. We will test each set of tuning parameters suggested by Aim 2B by testing the eleven predictions in Table 1[25]. Specifically, each muscle listed in column 1 of Table 1 is associated with a clear, testable prediction in column 2 of Table 1: *"X" muscle performs "Y" action*. If it does not, some other muscle or combination of muscles must be involved in generating the observed kinematics. The mystacial pad model allows us to selectively "lesion" muscles in simulation to test these 11 predictions. We will remove muscles in simulation to make predictions for behavioral deficits that would be observed were the lesions made in the real animal. Although these model predictions can be tested by performing muscle-detachment studies in awake behaving animals, we will make every effort to avoid doing these invasive experiments. Instead, we will first try to obtain estimates of the effects of lesions by exploiting the wide, natural variability in the magnitude of muscle activation (as monitored by EMG) that occurs across different behaviors. To make use of EMG signals, we will first obtain EMG recordings in each animal as it exerts maximal effort while whisking. Maximum whisking can be induced by presenting a novel olfactory stimulus, or by placing the animal in a completely dark, novel behavioral arena. All subsequent EMG recordings will then be normalized against this maximal effort value, yielding a (likely non-linear) relationship between EMG and force production over a wide variety of different behaviors and search patterns.

Aim 2C: Predicted outcomes, potential challenges, and alternatives: By the end of Aim 2C, which will have been performed iteratively with Aim 2B, we will have tuned and tested the relative muscle contributions to specific whisker motor patterns. The model will tell us about relative functional relationships between muscles during different whisking motions and behaviors. This modeling work will be challenging, but tractable, because once we have an initial model of the dynamics of the system, we can systematically select behavioral experiments that will generate the dynamic response that will allow us to best estimate the material parameters governing the system. For example, we may find that damping coefficients are best estimated from high frequency, low amplitude whisking. To achieve this dynamic response, we can induce "foveal whisking" by placing the scent of the home cage near the rat[123]. As a second example, we may find that the spring constants of the PMS and PMI (see Table 1) are best estimated by comparing different magnitudes of contraction. To achieve this mechanical behavior, we can record from these muscles while the rat is whisking while rotating its head; this will induce a large magnitude mystacial pad contraction on one side of the face, and a small amplitude contraction on the other[30, 34]. These types of experiments can help guarantee that our estimation procedures will converge. Finally, we note that even in the worst possible case – that two or more muscles exert completely non-independent forces on a follicles – we can selectively detach muscles from the skull to identify their unique actions. If needed, we could selectively sever the connection of the muscle to the bone for each of the extrinsic muscles except *nasolabialis profundis*, which attaches to the nasal cartilage near the philtrum. We will carefully monitor changes in motor strategies over time, as the rat recovers from the lesion. We can further tease apart muscle compensation from muscle reattachment (healing) by adhering a small bolus of sterile bone wax over the entheses during the detachment procedure. This will slow or prevent muscle reattachment.

Aim 3: Integrate 3D models of mystacial pad musculature with 3D models of vibrissal dynamics to perform experiments that close the vibrissal active-sensing loop. We combine the model developed in Aims 1 and 2 with our established models of vibrissal mechanics[36-44, 54, 55] to disentangle the relative roles of neural motor control and biomechanical constraint during different types of exploratory behavior. By integrating tactile feedback from the whiskers, we take a step towards closing the loop between motor action and the sensory data acquired. *Three specific hypotheses will be tested in the sub-aims.*

Overview of Aim 3: Two key ideas underlie the experiments proposed in Aim 3. First, the vibrissal system of the rodent is characterized by multiple "nested" feedback loops, all acting in parallel and involving multiple levels of the nervous system[1, 99]. The fastest reflex loop (~14 – 18 msec) processes tactile signals from the whisker through neurons of the trigeminal ganglion, trigeminal nuclei, and then directly to motor neurons of the facial motor nucleus that innervate the vibrissal muscles. Loops with an intermediate speed involve structures such as the superior colliculus, zona incerta, and the cerebellum, while the slowest loops involve both primary sensory and motor cortical areas[99]. These parallel nested loops will clearly induce different time scales at which whisking behaviors can be modulated, and they also form the basis for different degrees of voluntary vs. reflexive control. Second, these nested loops have recently been shown to incorporate central pattern generators (CPGs) for both whisking and sniffing[24, 62, 124, 125]. These CPGs are to some degree independent, and in other respects tightly locked. Vibrissal protraction is driven by a whisking oscillator located in the vibrissal zone of the intermediate band of the reticular formation (vIRt), while mystacial pad retraction is at least partly controlled by the respiratory CPG. Breathing can reset the whisking rhythm, but not vice-versa. The sub-aims below describe some experiments that will test specific hypotheses about the motor actions that subserve these complex neural circuits. In addition to the ones listed below, we will of course be guided by the new results of Aims 1 and 2, which will generate multiple novel hypotheses throughout the research program.

The experiments of Aim 3 will use only rats, as they are larger and easier to train. Equal numbers of adult male and female rats will be used in all experiments. Our laboratory's previous behavioral studies have used between 3 – 8 animals [34, 35, 51, 102, 118], and we anticipate similar numbers for each of the subaims below; numbers will be reduced if the same animal can be used in multiple experiments.

Aim 3A. Reflexive behaviors and their fast modulation. As described in *Toolset 3*, we recently demonstrated that the manner in which the whisker decelerates against objects will have a strong influence on the tactile signals generated at the whisker base[43]. Unintuitively, this effect is largely independent of the whisker's velocity at time of impact, instead depending almost entirely on the deceleration profile subsequent to the collision[43]. We will use the muscle models, coupled with our models of vibrissal dynamics[43, 54, 55] to quantify how much of the deceleration is biomechanically determined, compared with how much is volitionally controlled. Closely following the predictions of a previous behavioral study from the Ahissar laboratory[99], we will test the *hypothesis that fast acceleration changes immediately after collision result from an involuntary reflex loop, while longer latency changes in both ipsi- and contralateral contact profiles are determined by a voluntary sequence of motor actions*. Previous work[26, 27, 99] has shown that rats exhibit different responses between first whisk against an object (unexpected) and subsequent whisks (expected) as the animal gradually converges to a percept[126]. We will perform two-alternative forced choice experiments in which animals must discriminate the angle of a peg (vertical or tilted) placed at variable locations in an otherwise empty search space. For the first contacting whisk, regardless of peg orientation, we expect whisker dynamics to show a characteristic deceleration profile that depends only on dynamic state of the whisker at instant of contact. In contrast, we expect that subsequent whisks will exhibit more complex deceleration profiles, including contact-induced "double pumps." *Regardless of whether these data show the hypothesis to be correct*, we can compare whisker dynamics between first and subsequent whisks to explore the parameter space to determine the patterns of motor activation associated with tactile exploration. Variations on this experiment could involve adding a texture to the peg. These experiments will help reveal how choice of whisking strategies is determined by behavioral task.

Aim 3B. Voluntary, row-wise control over elevation and roll. There are multiple anatomical and physiological reasons to focus on the row as a fundamental unit of actuation. The most obvious reason is that the intrinsic muscles attach in rows. More intriguingly, however, the vibrissae of each row have been shown to undergo different magnitudes of roll and elevation[98]. Roll and elevation, in turn, both have an extremely large effect on the trajectories of the vibrissal tips[122]. Elevation, for example, causes the trajectories of the vibrissae tips to align with the pitch of the head, and reduces redundancy in the search space during a protraction, while roll differentially changes the path lengths of dorsal and ventral vibrissae[122]. Thus it is critical to determine whether the rat can selectively control these parameters. We will test the *hypothesis that – regardless of sensory task – roll and elevation are necessary biomechanical consequences of facial musculature, and* ***not*** *under volitional control.* This hypothesis is based on earlier studies[58] and on the schematic of Fig. 12, which shows that the S/L ratio determines whether different whiskers will move in a similar way in response to a given motor command. If this ratio remains constant within a row then whiskers will show similar angular motion in response to similar muscle contractions. If this ratio does varies within a row, then whiskers will show different angular motion in response to similar muscle contractions. Our preliminary analysis suggests that the S/L ratio remains relatively constant within a row, but changes across rows. We will test the rat on a battery of behavioral tasks established in our laboratory: searching empty space; localizing an object; discriminating objects; and localizing the direction

of airflow[34, 35, 51, 102, 118]. If our hypothesis is correct, we will find that in all conditions, elevation and roll are directly correlated with protraction amplitude, but this correlation will be weak if our hypothesis is incorrect. *Regardless of whether the hypothesis is correct*, we will be able to assess the degree to which intrinsic and extrinsic muscles *contribute to the differential movement of whiskers within and across rows.*

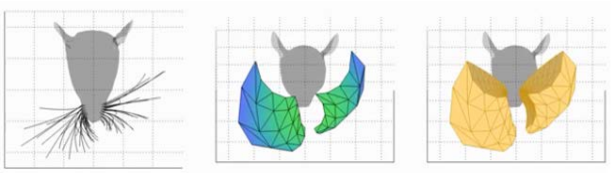

Fig. 14. Spread (left) measures the angle between rostral and caudal whiskers, which can differ bilaterally. It is a direct measure of the sensing space, measured by either surface area (center) or, volume (right). Data from Huet et al., 2015.

Aim 3C. Active control of sensing resolution. Previous studies have shown that two principal components capture most of the variations in whisking patterns during vibrissotactile exploratory behavior: the average protraction angle, and the "spread" of the array, defined as the angular difference between rostral and caudal whiskers[26]. The average vibrissal protraction angle is likely to reflect the animal's focus of attention, particularly during periods of contact with an object[26-30]. In addition, we recently demonstrated that the spread of the array is a direct measure of the animal's sensing space – either surface area of the whisker tips, or of the volume of the array (Fig. 14). A key finding of the same study was that sensing resolution does not change substantially with protraction angle, instead, it depends almost entirely on the spread of the array. *We will test the hypothesis that intrinsic muscles exert differential control over rostral and caudal whisk amplitude against the alternative that extrinsic muscles change the shape of the mystacial pad to bring the whiskers closer together*. To test this hypothesis, we will carefully monitor whisker spread during a set of sensory discrimination tasks and simulate the sensory data obtained. We will test whether activation of the intrinsic or extrinsic muscles is better correlated with periods of high resolution sensory-data acquisition. *Regardless of whether the hypothesis is correct or incorrect*, or whether both mechanisms are found to work in concert, the results of the experiment will directly constrain the neural commands required to change the rat's search space and location.

Aim 3D.The role of co-contraction during high-resolution exploration. In addition to generating rhythmic motion, co-contraction of muscles in the mystacial pad can provide varying degrees of rigidity against which the follicle can move. We expect that during high-resolution exploratory behaviors (e.g., foveal whisking against an object) the rat will co-contract its muscles in a manner so as to resist follicle rotation. An open question is whether the rigidity associated with co-contraction can be achieved at different protraction angles, or whether rigidity requires the whiskers "stuck" near full protraction (as is often observed during the sniffing behavior associated with rearing). We will run simulations to test how mystacial pad compliance varies as muscles are co-contracted to varying degrees, and compare against behavioral results.

Aim 3E. Coordination with sniffing. Recent work has identified the whisking "central pattern generator" and shown that the breathing rhythm influences the whisking rhythm but not vice versa [24, 62, 124, 125]. We will perform experiments in which we disrupt the rat's breathing cycle with ammonia[24]to identify the patterns of muscle activation specifically associated with the coupled breathing-whisking cycle. By then adding tactile feedback on select trials, we can begin to identify biomechanical constraints that can help distinguish the extent to which the whisking CPG is gated by higher-order centers, compared to the role of tactile feedback in altering the phase relation between the whisking and breathing muscles.

Aim 3: Predicted outcomes, potential challenges, and alternatives: **By the end of Aim 3** Although behavioral experiments are always challenging, our laboratory has extensive experience in this area[34, 35, 51, 102, 118], including a recent experiment in which we successfully trained rats on 5-alternative forced choice task[118]. We will be very careful to ensure that all experiments in Aim 3 will yield useful results regardless of whether particular hypotheses are shown to be correct or incorrect. A final challenge we anticipate is that the rostral muscles that control the nares are quite complicated. We are aided by a two recent studies that describes them in detail[56, 62] The work clearly distinguishes the muscles involved in sniffing from the muscles involved in vibrissal movement.

TIMELINE

Year / Task	Year 1				Year 2				Year 3				Year 4				Year5			
	q1	q2	q3	q4	q1	q2	q3	q4	q1	q2	q3	q4	q1	q2	q3	q4	q1	q2	q3	q4
Aim 1	Aim 1 and Aim 2 iterate																			
Aim 2A																				
Aim 2B						Aim 2B and 2C iterate														
Aim 2C																				
Aim 3																				

No *biohazards or select agents* are used. No *foreign organizations* are involved. *Relevant biological variables:* Variability due to age and genetic background will be controlled by using age-matched littermates for all comparisons. Equal numbers of male and female animals will be used in each experiment. *Authentication of Key Biological and/or Chemical Resources:* N/A.